Published in final edited form as:
Cancer Gene Ther. 2009 July ; 16(7): 551–560. doi:10.1038/cgt.2009.10.

Oncolytic herpes simplex virus vectors and taxanes synergize to promote killing of prostate cancer cells

BJ Passer, **P Castelo-Branco**, **JS Buhrman**, **S Varghese**, **SD Rabkin**, and **RL Martuza**
Department of Neurosurgery, Massachusetts General Hospital and Harvard Medical School, Boston, MA, USA

Abstract

Genetically engineered oncolytic herpes simplex virus-1 (HSV-1) vectors selectively replicate in tumor cells causing direct killing whereas sparing normal cells. One clinical limitation of using oncolytic HSV vectors is their attenuated growth. We hypothesized that the appropriately chosen chemotherapeutic agent combined with an oncolytic HSV could be an effective means to promote augmented prostate cancer cell killing both *in vitro* and *in vivo*. Here we have identified that G47Δ synergizes with the microtubule-stabilizing taxane agents docetaxel and paclitaxel to enhance the *in vitro* killing of prostate cancer cells. *In vivo* efficacy studies show that when combined with docetaxel, G47Δ could be reduced at least 10-fold. Immunoblot analysis revealed that docetaxel-induced accumulation of the phospho-specific mitotic markers op18/stathmin or histone-H3 was markedly reduced by G47Δ, which correlated with enhanced apoptosis and required active viral replication. Furthermore, cell-cycle analysis demonstrated that in the presence of G47Δ, the majority of 4N cells arrested in mitosis were MPM-2-negative, indicative of cells exiting mitosis prematurely. These findings suggest that G47Δ may act in part, on mitotically blocked cells to enhance cell death, which may account for the enhanced antitumor efficacy observed *in vivo*.

Keywords

prostate cancer; oncolytic HSV's; taxanes

Introduction

Viral vectors genetically engineered for replication competence restricted to cancer cells represent an attractive strategy for tumor-based therapies because they can replicate and spread *in situ*, exhibiting oncolytic activity through direct cytopathic effects. These lytic viruses offer a distinct advantage over other forms of cancer therapies in that they are self-perpetuating and can spread not only in the tumor itself but also to distant micrometastases. G47Δ represents a newer generation replication-competent HSV-1 vector based on G207 with an additional deletion within the nonessential *α47* gene.[1] The deletion of *α47* not only prevents downregulation of major histocompatibilty complex class I but also places the late *US11* gene under the control of the immediate early *α47* promoter. This alteration of *US11* expression enhances the growth of G47Δ by precluding the shutoff of protein synthesis.[2,3] G47Δ has been demonstrated to be more effective than G207 in promoting tumor regression in xenogenic models of both brain and prostate cancers.[1,4]

Correspondence: Dr BJ Passer, Brain Tumor Research Center, Neurosurgery Department, Massachusetts General Hospital, Simches Research Building CRPZN 3800, 185 Cambridge Street, Boston, MA 02114, USA. bpasser@partners.org.

HSV vectors are nontoxic to normal prostate and the surrounding nerves following intraprostatic inoculation in mice and nonhuman primates.[5] In addition, HSV mutants are effective against human prostate cancer irrespective of hormone status or radiosensitivity, a major advantage in its application for advanced forms of the disease, where hormone and radiation refractory tumor is common.[4,6] Moreover, HSV mutants can elicit a tumor-specific host immune response by acting as an *in situ* vaccine thereby making them potentially attractive for treating metastatic prostate cancer.[7–9]

As herpes-derived oncolytic vectors are attenuated, which can decrease replication and spread in certain tumors and limit their overall antitumor efficacy, we hypothesized that appropriately chosen chemotherapeutic agents combined with oncolytic HSV vectors would improve antitumor efficacy. We have determined that taxanes, such as docetaxel and paclitaxel, when combined with G47Δ promote increased cell death in prostate cancer cells in a synergistic manner. Both docetaxel and paclitaxel have been used in phase II/III clinical trials against a variety of solid tumors including prostate cancer.[10] These spindle poisons bind to and stabilize microtubules resulting in mitotic arrest. However, cells do not generally undergo G_2/M arrest at low taxane concentrations, but die of aberrant mitosis resulting from the formation of multipolar spindles and an aneuploid G_1 population of cells.[11] At higher drug concentrations, cells are arrested at mitosis, but if mitotic arrest cannot be sustained due to the activation of the spindle assembly checkpoint, mitotic slippage may occur resulting in mitotic exist without cytokinesis.[12,13]

α-Herpesviruses also impair cell-cycle progression but do so in a manner that is distinctly different from taxanes. HSV infection results in host-cell growth arrest at the G_1-phase of the cell cycle.[14,15] The HSV-1 proteins ICP27, ICP0 and ICP4 contribute to the G_1 arrest,[16] which are not deleted in G47Δ.[1] As HSV-1 and taxanes differentially affect the cell cycle either by arresting cells at G_1 or mitosis, respectively, we suspected that their combination might result in a productive synergy resulting in enhanced prostate cancer cell killing.

Materials and methods

Cells and chemotherapeutic agents

LNCaP cells were grown in RPMI medium containing 10% heat-inactivated fetal calf serum (Hyclone, Logan, UT), 1mM sodium pyruvate, 10mM hepes buffer and 100Uml^{-1} penicillin-streptomycin. Vero and DU145 cells were grown in Dulbecco's modified Eagle's medium supplemented with 10% calf serum. Human prostate epithelial cells and its culture medium PrEGM were obtained from Cambrex and maintained as described by the manufacturer. Cells were cultured at 37 °C and 5% CO_2. The compounds used in this study included, Paclitaxel (Bristol-Myers Squibb, Princeton, NJ), docetaxel (Aventis Pharmaceuticals Inc., Bridgewater, NJ), cisplatin (Sigma, St Louis, MO), doxorubicin (Pharmacia and Upjohn Company, Kalamazoo, MI) and etoposide (Bristol-Myers Squibb).

Viruses

The HSV-1 strain G47Δ, which was derived from G207 (γ34.5$^-$, ICP6$^-$, *LacZ*$^+$;17), was generated by deletion of the *47* gene and the promoter region of the *US11* gene.[1] Wild-type HSV-1 strain, Strain F, was obtained from Bernard Roizman, (University of Chicago, Chicago, IL).

Cell susceptibility assays and Chou–Talalay analysis

LNCaP and DU145 cells were seeded into 96-well plates at 2000 cells per well. For cell-susceptibility assays, G47Δ at a multiplicity of infection (MOI) of 0.01 (LNCaP) or 0.05 (DU145 cells) and the indicated compound concentrations were added alone or in combination.

Seventy-two hours after infection, MTSassays (Promega, Madison, WI) were performed according to the manufacturer's instructions. For Chou–Talalay analysis, dose–response curves and 50% effective dose values (ED_{50}) were obtained and compared at day 4. For ED_{50} determination, cells were incubated for 4 days with varying concentrations or MOIs of drug and virus, respectively, and cell survival was then assessed using MTSassays. Dose–response curves were fit to Chou–Talalay lines, which are derived from the law of mass action and are described by the equation $\log(f_a/f_u)=m \log D - m \log D_m$, in which f_a is the fraction affected (percent cell death), f_u is the fraction unaffected (percent cell survival), D is the dose, D_m is the median-effect dose (the dose causing 50% of cells to be affected, that is, 50% survival), and m is the coefficient signifying the shape of the dose–response curve.

The combination index (CI)-isobologram by Chou and Talalay[18] was used to analyze virus and drug combinations. Fixed ratios of virus and drug concentrations and mutually exclusive equations were used to determine CIs. All experiments were repeated at least three times.

Single-step growth and cell-free virus assays

LNCaP cells either remained untreated or were pretreated with either docetaxel or paclitaxel (0.025–0.2 nM) for 12 h and thereafter, cells were infected with G47Δ at an MOI of 1.5. At 24 or 48 h after infection, cells were scraped into the medium and subjected to three freeze-thaw cycles. Virus titers were determined by plaque assays on Vero cells. Each concentration in an experiment was plated in duplicate, and each experiment was performed three times. For cell-free virus assays, supernatants and cell lysates were titered separately on Vero cells.

In vivo studies

All procedures were approved by the MGH Subcommittee on Research Animal Care. LNCaP cells (5×10^6 cells) were implanted subcutaneously into the flanks of 6- to 8-week-old athymic male mice (n=5–8 mice per group). Tumor volume was calculated using the formula width $(\text{mm})^2\times\text{length (mm)}\times0.52$.

PSA ELISA

Blood was collected via the facial vein and allowed to clot at room temperature. prostate-specific antigen (PSA) levels were determined using a PSA ELISA kit (American Qualex Antibodies, San Clemente, CA.).

Immunoblots

LNCaP cells (75 000 per well) were treated with G47Δ (MOI 0.1 or 1), docetaxel (1 or 10 nM) or the indicated combinations for up to 48 h. Cells pellets were lysed in RIPA buffer plus a cocktail of protease and phosphatase inhibitors (Boston Bioproducts, Worcester, MA). The following antibodies were used: anti-phospho-op18 (Ser16; Santa Cruz Biotechnology, Santa Cruz, CA), anti-stathmin-1 (Abcam, Cambridge, MA), anti-caspase-3 (Cell Signaling Technology, Danvers, MA), anti-PARP (Trevigen, Gaithersburg, MD), anti-phospho-histone-H3 (Upstate, Lake Placid, NY), anti-tubulin (Sigma), anti-phospho- eIF2α (Ser51) and anti-eIF2α (Cell Signaling Technology). Membranes were then probed with peroxidase- conjugated secondary antibodies (Promega) and protein bands were visualized by enhanced chemiluminescence (Amersham Biosciences, Piscataway, NJ).

Flow cytometric analysis of the cell cycle

LNCaP cells were seeded into 10 cm dishes at 7.5×10^5 cells per plate and treated with either G47Δ (MOI 1), docetaxel (10 nM) or their combination. At the indicated time points, cells were pelleted, fixed in 70% ethanol and stored at −20 °C. Before analysis, fixed cells were washed twice in phosphate-buffered saline (PBS) containing bovine serum albumin (0.5%)

and EDTA (20mM), stained with anti-MPM-2 antibody (R&D Systems, Minneapolis, MN) followed by a secondary antibody conjugated fluorescein isothyocyanate (Southern Biotechnology, Birmingham, AL). Labeled cells were resuspended in a propidium iodide (PI) (50 $\mu g ml^{-1}$; Sigma) solution containing 0.1% sodium citrate, 0.1% Triton-X and 2 $\mu g ml^{-1}$ RNase A (Sigma) and immediately analyzed by flow cytometry on a BD FACSCalibur instrument as previously described.[19] Data was analyzed using Flowjo software (Ashland, OR).

In vitro analysis of apoptotic bodies and *in vivo* analysis of phospho-histone H3 positive cells

LNCaP cells were grown overnight in eight-well chamber slides (Nalgene, Naperville, IL) and treated with G47Δ (MOI 1) alone, docetaxel (10 nM) alone or their combination. Approximately 36 h after treatment, cells were fixed in 4% paraformaldehyde (Electron Microscopy Sciences, Fort Washington, PA), washed in PBSand mounted in media containing 4′,6-diamidino-2-phenylindole dihydrochloride (DAPI; Vector, Burlingame, CA). Percentage of micronuclei-containing cells per field view (>40 field views per condition) was determined in three separate experiments. For phospho-histone H3 positive (p-$H3^+$) cell analysis, tumors were removed one day following the last docetaxel injection, embedded in optical coherence tomography and immediately frozen in liquid nitrogen-cooled *N*-methybutane. Tumor sections (5 μM) for each of the treatment groups (n=3 per group) were double stained with an anti-p-H3 antibody and DAPI. Tumor cells were quantified from at least 10 random fields of view per tissue sample. More than 150 cells were counted for each variable per experiment. A Nikon E800 epifluorescence microscope was used to perform the analysis using a ×20 objective.

Statistical analysis

For comparison of cell susceptibility assays, *in vivo* efficacy studies and mechanism of efficacy, Student's *t*-test (two-tailed) was used to analyze significance between two treatment groups using GraphPad Prism v.4 (San Diego, CA).

Results

G47Δ and taxanes promote killing of LNCaP prostate cancer cells in a synergistic manner

We initially screened *in vitro* several FDA-approved chemotherapeutics in conjunction with the HSV-derived oncolytic virus G47Δ to determine whether a specific combination resulted in augmented killing of prostate cancer cells as compared to either one alone. Cell susceptibility assays were performed on LNCaP and DU145 cells, which were incubated with increasing concentrations of the indicated chemotherapeutic agent either alone or in combination with G47Δ. This analysis indicated that the combination of G47Δ together with either docetaxel or paclitaxel, two taxane family members that stabilize microtubules, significantly increased prostate cancer cell killing (Figures 1d–f). By contrast, doxorubicin, etoposide and cisplatin, did not significantly enhance cell killing when paired with G47Δ (Figures 1a–c). Overall, these results show that the combination of G47Δ and taxanes result in increased cell killing as compared to either one alone.

To extend these findings, CI methods of Chou–Talalay were used to determine whether G47Δ in conjunction with either docetaxel or paclitaxel could promote LNCaP cell killing in a synergistic manner. By definition, a CI value of 1 indicates an additive effect, whereas CI>0.9 and CI>1.1 indicate synergism or antagonism, respectively. The ED_{50} of G47Δ (MOI 0.07), docetaxel (0.85 nM) and paclitaxel (2.8 nM) were determined for LNCaP cells. Figure 1g shows that as a function of the f_a, synergism was observed for the combination of G47Δ and either docetaxel or paclitaxel, whereas the combination of G47Δ with either doxorubicin (ED_{50}=56.2 nM), etoposide (ED_{50}=6.1 μM) or cisplatin (ED_{50}=8.6 μM) did not result in synergistic killing of LNCaP cells (Figure 1h). Synergy was also observed for certain f_a (<0.8) for the combination

of G47Δ (ED_{50}=0.7) and either docetaxel ($ED_{50=}$1.48 nM), paclitaxel (ED_{50}=3.13 nM) on DU145 cells. In addition, Chou–Talalay analysis also demonstrated that the combination of G47Δ with either docetaxel or paclitaxel on normal prostate epithelial cells derived from primary cultures resulted in CI values that reflected an antagonistic effect for all fraction-affected points tested (data not shown). Overall, these data show that oncolytic HSV and taxanes can combine to promote synergistic of killing of prostate cancer cells but not in normal prostate epithelial cells.

Taxanes do not affect the replication of G47Δ

Previously, it was shown that taxanes could increase adenovirus replication, which was proposed to account for the synergy observed between the CV787 vector and docetaxel.[20] Therefore, single-step growth curve assays were performed to assess whether the augmented LNCaP cell killing was due in part, to enhanced G47Δ replication by docetaxel. Twelve hours pretreatment with nontoxic concentrations of docetaxel (0.025–0.2 nM) neither increased nor decreased viral titers as compared to G47Δ alone at 24 and 48 h after infection in single-step growth curve assays (Figures 2a and b, respectively). In addition, cell-free virus assays were performed to determine whether taxanes might affect virus egress from the cell. By 48 h after infection, no differences in G47Δ titers from LNCaP-derived supernatants were observed between the different treatment groups (Figure 2c). Finally, X-gal staining of LNCaP cells infected with G47Δ (ICP6 is replaced with *LacZ*) at a MOI of 0.1 also confirmed that pretreatment with the indicated concentrations of docetaxel had minimal influence on G47Δ spread (Figure 2d).

G47Δ and docetaxel combination therapy promotes tumor regression in LNCaP xenografts

Next, we evaluated the *in vivo* antitumor efficacy of G47Δ and docetaxel separately and in combination. Initially, antitumor efficacies of individual therapies were established to determine treatment conditions resulting in tumor size reductions of ~30–50% (data not shown). Tumor-bearing mice were administered mock control, G47Δ at 2×10^4 or 2×10^5 pfu (q3d×2), docetaxel at 3mgkg^{-1} (q3d×3) or both G47Δ and docetaxel. For combination therapy, G47Δ was inoculated on days 0 and 3, and the following day (day 4), mice received docetaxel, which was repeated every third day for a total of three injections. Figure 3a illustrates that by day 47 after tumor implantation, a statistically significant decrease in tumor volume was observed between control (942±102.6mm^3; n=5) and all of the treatment groups. In particular, treatment with G47Δ at 2×10^4 pfu resulted in a notable reduction in tumor size (416±49mm^3; n=7), whereas a log-fold increase in G47Δ resulted in a larger reduction in tumor growth (144.4 ±12.5mm^3; n=5). Three intraperitoneal injections of docetaxel at 3mg kg^{-1} also resulted in partial tumor regression (627mm^3±51.7; n=6). Importantly, lowering the dose of G47Δ 10-fold combined with docetaxel was equally as effective as G47Δ 2×10^5 pfu alone. These results demonstrate that when combined with docetaxel, G47Δ can be reduced at least 10-fold to achieve levels of tumor reduction comparable to a G47Δ at 2×10^5 pfu. It was also noted that G47Δ and docetaxel promoted reduced tumor weight and reduced PSA levels as compared to the other treatment groups (Figures 3b and c, respectively). Lastly, this combination therapy regime appeared to be nontoxic to mice, because their body weight remained relatively stable throughout the course of the study (Figure 3d).

G47Δ impairs docetaxel-mediated op18/stathmin and histone-H3 phosphorylation

Initially, we assessed the consequences of G47Δ infection on docetaxel-induced mitotic arrest by immunoblotting for two commonly used markers of mitosis, phospho-op18/stathmin or p-H3. To this end, LNCaP cells were treated either with G47Δ at a MOI of 0.1 or 1, docetaxel at 1 or 10 nM or simultaneously with the indicated combinations. As expected, treatment with 10 nM of docetaxel for 48 h resulted in the appearance of a prominent 23 kDa band recognized

by the phospho-specific op18/stathmin antibody. Although docetaxel in combination with G47Δ at a MOI of 0.1 mildly affected the level of phosphorylation of op18/stathmin, G47Δ at a MOI of 1 substantially decreased the intensity of this band (Figure 4a). Probing with an antibody that recognizes both phosphorylated and nonphosphorylated forms of op18/stathmin further confirmed these results. Although nonphosphorylated levels of op18/stathmin remained unchanged in each of the experimental conditions, phosphorylated op18/stathmin mirrored the results obtained using the phospho-specific op18/stathmin antibody (Figure 4a). Thus, it appears that docetaxel-induced phosphorylation of op18/stathmin in LNCaP cells is attenuated by G47Δ. In addition, combination treatment of G47Δ (MOI 1) and docetaxel (10 nM) also produced a notable increase in the cleavage of full-length caspase-3 and PARP, reflecting increased apoptosis. Next, we examined the temporal-dependent consequences of G47Δ on docetaxel-mediated op18/stathmin phosphorylation. Figure 4b shows that op18/stathmin is phosphorylated as early as 12 h following treatment with docetaxel (10 nM) and persists in the presence of G47Δ (MOI 1) for at least 24 h. However, by 48 h after infection, nearly complete elimination of the phosphorylated form of op18/stathmin was observed. Moreover, we determined that the effect of G47Δ on docetaxel-induced op18/stathmin phosphorylation is dependent on viral replication, because pretreatment with acyclovir, a commonly used anti-herpetic agent used to block viral replication, greatly attenuated this effect (Figure 4c). Concomitantly, we verified the activity of acyclovir on G47Δ replication by performing single-step growth curve assays (Figure 4d). Importantly, we also validated the above findings by immunoblotting with the anti-p-H3 antibody, which mirrored the results obtained with anti-phospho-op18/stathmin (Figure 4c). Control experiments were performed to demonstrate that G47Δ replication does not globally impair protein phosphorylation in the presence of docetaxel. HSV-1 infection enhances eIF2α phosphorylation, [21] but should not be influenced by docetaxel. As anticipated, immunoblot analysis showed that eIF2α enhanced phosphorylation by G47Δ was not altered by the presence of docetaxel (Figure 4c).

Accumulation of MPM-2$^+$ cells promoted by docetaxel is compromised by G47Δ

To further assess the effect of G47Δ on mitotically blocked LNCaP cells, cell-cycle analysis was performed using two-color PI and anti-MPM-2 staining. The anti- MPM-2 antibody specifically labels cells in mitosis. Although docetaxel (10 nM)-induced mitotic arrest peaked by 24 h as demonstrated by the accumulation of cells with increased 4N DNA content and MPM-2 labeling (Figure 4e), the addition of G47Δ (MOI 1) resulted in a notable decrease the percentage of MPM-2$^+$ cells. By 36 h, the effect G47Δ on docetaxel-arrested cells was more evident, resulting in a substantial diminution in MPM-2 labeling. This decrease was not the result of a general decrease in 4N DNA content, because infection with G47Δ resulted in a 44% reduction in the 4N population a compared to a 92% diminution of MPM-2$^+$ cells. As shown in Figure 4f, analysis of 4N-gated cells revealed that by 24 h and more strikingly by 36 h, the majority of the 4N population lacked MPM-2 labeling in the presence of G47Δ, indicative of cells undergoing premature mitotic exit.

In vitro and *in vivo* consequences of G47Δ and docetaxel combination treatment

To characterize the morphological features of LNCaP cells treated with G47Δ (1 MOI), docetaxel (10 nM) or their combination, we examined DAPI-stained nuclei of these cells by fluorescent microscopy after 36 h of treatment (Figure 5a). Docetaxel treatment resulted in 10.4±1.9% of the cells containing fragmented nuclei, whereas the combined treatment of G47Δ and docetaxel increased this effect (17±2.2%; Figure 5b). In addition, we observed that cells containing fragmented nuclei lacked MPM-2 labeling (data not shown).

These studies were also extended to an *in vivo* analysis of LNCaP tumors. We scored the number of mitotic cells as a function of treatment groups for three mice per group (Figure 5a). LNCaP xenografts were treated in an identical fashion as described for the results obtained in

Figure 2. Two days following the last treatment with docetaxel, tumor sections were immunostained with the anti-p-H3 antibody and p-H3$^+$ cells were scored for each of the treatment groups (Figure 5c). Our analysis indicated that as expected, docetaxel alone significantly increased the number of p-H3$^+$ cells (25.7%±4.6 compared to 13.7%±2.9 for mock control). However, administration of G47Δ in combination with docetaxel diminished the number of p-H3$^+$ cells to similar extent as compared to mock or G47Δ alone.

Discussion

Replication-competent HSV vectors, such as G47Δ, are attenuated, which can diminish overall viral replication and spread within the tumor mass. As these viruses kill tumors by oncolytic mechanisms, which are different from standard anticancer therapies, we hypothesized that an appropriately chosen chemotherapeutic agent used in a combination therapy approach would permit for greater prostate cancer cell killing. In this study we identified the combination of G47Δ and taxanes that is, docetaxel or paclitaxel, to synergize, thereby enhancing prostate cancer cell killing.

The use of oncolytic HSVs in combination with chemo-, radio- or gene-therapy approaches is well documented.[22] With regard to chemotherapeutic approaches, a number of established modalities have been used together with HSV mutants that not only kill malignant cells but have also been shown to predispose these cancerous cells towards increased viral replication by changing the balance of cellular RR and GADD34. For example, G207 has been used in combination with temozolamide and fluorodeoxyuridine (FUdR) to treat gliomas and colorectal cancer, respectively.[23,24] Temozolamide and FUdR treatments increase either cellular RR or GADD34 protein levels resulting in greater viral replication and increased antitumor efficacy. 5-FU and gemcitabine have also been shown to potentiate the efficacy of G207 replication in pancreatic cancers.25 Other HSV mutants have been created to take advantage of targeting other specific cellular pathways. For example, the HSV US3$^-$ mutant synergizes with phosphatidylinositol 3-kinase-akt inhibitors by increasing intracellular AKT activity.[26]

Our data indicate that chemotherapeutic-mediated enhancement of viral replication is not the mechanism of action responsible for the observed increased in prostate cancer cell killing. Pretreatment of prostate cancer cells with nontoxic doses of either docetaxel or paclitaxel neither increased nor decreased G47Δ replication. Accordingly, our data suggest that the observed augmented cell killing is due to cell-cycle-specific effects imposed by taxanes and HSV-1. We initially observed by immunoblotting that G47Δ infection abolished the appearance of the phosphorylated species of op18/stathmin and histone-H3 induced by docetaxel. This phenomenon appeared to be dependent on active viral replication because acyclovir, a potent antiherpetic drug, maintained the appearance of these mitotic markers.

4N DNA content constitutes both nonmitotic (that is, G_2) and mitotic (that is, M cell) populations. To determine whether G47Δ effects mitotically arrested cells promoted by docetaxel, PI and MPM-2 dual labeling was performed. By 24 h after docetaxel treatment, the majority of cells were composed of 4N DNA (~78%) and MPM-2 labeling (~66%), indicative of mitotic arrest. By 36 h, the MPM-2-containing population had decreased to ~42%, which is indicative of cells undergoing mitotic slippage. Mitotic slippage occurs when cells exit mitosis without having satisfied their spindle assemble checkpoint, that is, mitosis and subsequent cell division despite nonfunctional spindles.[27] Consistent with our immunoblot data, combination treatment resulted in a substantial decrease in MPM-2$^+$ population, which was particularly evident by 36 h. This decrease is not likely the result of a general decrease in the 4N DNA content because infection with G47Δ resulted in only ~44% reduction in 4N DNA content as compared to a ~92% diminution for MPM- 2$^+$ cells. These data suggest that although

G47Δ and docetaxel can independently affect different phases of the cell cycle to eventually promote cell death, G47Δ may also act on mitotically arrested cells to enhance this affect.

The concept of an oncolytic HSV and taxane combination approach for prostate cancer is novel from both a therapeutic perspective as well as from a mechanistic point of view. With regard to the latter, our data are reminiscent of previously published work describing robust tumor cell killing by mechanisms that disrupt different phases of the cell cycle using a two-drug combination approach. Motwani *et al*., reported that the combination of flavopiridol, a cyclin-dependent kinase inhibitor that arrests cells at the G_1/Sboundary of the cell cycle together with paclitaxel, promoted a strong synergistic apoptotic response in both human breast and gastric cancer cell lines.[28] Flavopiridol was shown to accelerate mitotic exit when it followed paclitaxel administration and that this effect was associated with diminished levels of the mitotic markerMPM-2. Other studies have shown that flavopiridol combined with epothilone-B (EpoB), a nontaxane microtubule-stabilizing agent in MB-468 and SKBR-3 breast cancer cells promoted a robust apoptotic response.[29] Similar effects were also noted when docetaxel was substituted for EpoB. Similarly, purovalanol A, a Cdk1 inhibitor was shown to accelerate mitotic slippage promoted by the antimitotic agent KSP-1A as well as paclitaxel, which resulted in the marked depletion of p-$H3^+$ cells.[30] Finally, in agreement with our findings, it was recently shown that the combination of G207 and paclitaxel synergized to promote enhanced thyroid cancer cell killing.[31] It was proposed that like paclitaxel, G207 can also stabilize microtubules, that is, by increasing acetylated α-tubulin, and therefore, a G207 and paclitaxel combination would lead to increased microtubule stabilization and cell death.

In summary, these data have important clinical implications for the treatment of prostate cancer. Both taxanes and oncolytic HSVs have been used separately with safety in clinical trials and the combination would appear to be readily adapted clinical trials in prostate cancer. Moreover, these data underscores the importance of exploring pathways common to pharmacological agents and oncolytic viruses for synergistic interactions and thus opens an avenue of exploration of mechanisms that are important to other cancers and other small molecules and related pharmaceuticals.

Acknowledgments

We thank Dr Martin Gullberg (Umeå University, Sweden) and Dr Patricia Schaffer (Harvard Medical School, Boston, MA) for very helpful advice and insightful discussions, and Melissa Marinelli for technical support with the mice studies. Fluorescent microscopy was performed in the Microscopy Core of the Program in Membrane Biology, which receives additional support from an Inflammatory Bowel Disease Center Grant DK43351 and a Boston Area Diabetes and Endocrinology Research Center Award DK57521. This study was in part supported by a grant to RLM (RO1 CA102139).

References

1. Toda T, Martuza RL, Rabkin SD, Johnson PA. Oncolytic herpes simplex virus vector with enhanced MHC class I presentation and tumor cell killing. Proc Natl Acad Sci USA 2001;98:6396–6401. [PubMed: 11353831]
2. He B, Chou J, Brandimarti R, Mohr I, Gluzman Y, Roizman B. Suppression of the phenotype of gamma (1)34.5-herpes simplex virus 1: failure of activated RNA-dependent protein kinase to shut off protein synthesis is associated with a deletion in the domain of the alpha47 gene. J Virol 1997;71:6049–6054. [PubMed: 9223497]
3. Cassady KA, Gross M, Roizman B. The second-site mutation in the herpes simplex virus recombinants lacking the gamma134.5 genes precludes shutoff of protein synthesis by blocking the phosphorylation of eIF-2alpha. J Virol 1998;72:7005–7011. [PubMed: 9696792]
4. Fukuhara H, Martuza RL, Rabkin SD, Ito Y, Toda T. Oncolytic herpes simplex virus vector g47delta in combination with androgen ablation for the treatment of human prostate adenocarcinoma. Clin Cancer Res 2005;11:7886–7890. [PubMed: 16278413]

5. Varghese S, Newsome JT, Rabkin SD, McGeagh K, Mahoney D, Nielsen P, et al. Preclinical safety evaluation of G207, a replication-competent herpes simplex virus type 1, inoculated intraprostatically in mice and nonhuman primates. Hum Gene Ther 2001;12:999–1010. [PubMed: 11387063]
6. Walker JR, McGeagh KG, Sundaresan P, Jorgensen TJ, Rabkin SD, Martuza RL. Local and systemic therapy of human prostate adenocarcinoma with the conditionally replicating herpes simplex virus vector G207. Hum Gene Ther 1999;10:2237–2243. [PubMed: 10498254]
7. Toda M, Martuza RL, Kojima H, Rabkin SD. *In situ* cancer vaccination: an IL-12 defective vector/replication-competent herpes simplex virus combination induces local and systemic antitumor activity. J Immunol 1998;160:4457–4464. [PubMed: 9574551]
8. Varghese S, Rabkin SD, Nielsen PG, Wang W, Martuza RL. Systemic oncolytic herpes virus therapy of poorly immunogenic prostate cancer metastatic to lung. Clin Cancer Res 2006;12:2919–2927. [PubMed: 16675589]
9. Varghese S, Rabkin SD, Liu R, Nielsen PG, Ipe T, Martuza RL. Enhanced therapeutic efficacy of IL-12, but not GMCSF, expressing oncolytic herpes simplex virus for transgenic mouse derived prostate cancers. Cancer Gene Ther 2006;13:253–265. [PubMed: 16179929]
10. Wilson L, Jordan M. Microtubules as a target for anticancer drugs. Nat Rev Cancer 2004;4:253–265. [PubMed: 15057285]
11. Chen JG, Horwitz SB. Differential mitotic responses to microtubule-stabilizing and—destabilizing drugs. Cancer Res 2002;62:1935–1938. [PubMed: 11929805]
12. Chen JG, Hang Yang C-P, Cammer M, Horwitz SB. Gene expression and mitotic exit induced by microtubule-stabilizing drugs. Cancer Res 2003;63:7891–7899. [PubMed: 14633718]
13. Castedo M, Perfettini JL, Roumier T, Andreau K, Medema R, Kroemer G. Cell death by mitotic catastrophe: A molecular definition. Oncogene 2004;23:2825–2837. [PubMed: 15077146]
14. Ehmann GL, McLean TI, Bachenheimer SL. Herpes simplex virus type 1 infection imposes a G1/Sblock in asynchronously growing cells and prevents G1 entry in quiescent cells. Virology 2000;267:335–349. [PubMed: 10662629]
15. Olgiate J, Ehmann GL, Vidyarthi S, Hilton MJ, Bachenheimer SL. Herpes simplex virus induces intracellular redistribution of E2F4 and accumulation of E2F pocket protein complexes. Virology 1999;258:257–270. [PubMed: 10366563]
16. Song BY, Yeh K-C, Liu J, Knipe DM. Herpes simplex virus gene products required for viral inhibition of expression of G1-phase functions. Virology 2001;290:320–328. [PubMed: 11883196]
17. Mineta T, Rabkin SD, Yazaki T, Hunter WD, Martuza RL. Attenuated multi-mutated herpes simplex virus-1 for the treatment of malignant gliomas. Nat Med 1995;1:938–943. [PubMed: 7585221]
18. Chou TC, Talalay P. Quantitative analysis of dose-effect relationships: the combined effects of multiple drugs or enzyme inhibitors. Adv Enzyme Regul 1984;22:27–55. [PubMed: 6382953]
19. Motwani M, Xiao-kui L, Schwartz GK. Flavopiridol, a cyclin-dependent kinase inhibitor, prevents spindle inhibitor-induced endoreduplication in human cancer cells. Clin Cancer Res 2000;6:924–932. [PubMed: 10741717]
20. Yu D-C, Chen Y, Dilley J, Li Y, Embry M, Zhang H, et al. Antitumor synergy of CV787, a prostate cancer-specific andenovirus, and paclitaxel and docetaxel. Cancer Res 2001;61:517–525. [PubMed: 11212244]
21. Chou J, Chen JJ, Gross M, Roizman B. Association of a M(r) 90 000 phosphoprotein with protein kinase PKR in cells exhibiting enhanced phosphorylation of translation initiation factor eIF-2 alpha and premature shutoff of protein synthesis after infection with gamma 134.5- mutants of herpes simplex virus 1. Proc Natl Acad Sci USA 1995;98:6396–6401.
22. Post DE, Fulci G, Chiocca EA, Van Meir EG. Replicative oncolytic herpes simplex viruses in combination cancer therapies. Curr Gene Ther 2004;4:41–51. [PubMed: 15032613]
23. Petrowsky H, Roberts G, Kooby DA, Burt BM, Bennett JJ, Delman KA, et al. Functional interaction between fluorodeoxyuridine- induced cellular alterations and replication of a ribonucleotide reductase-negative herpes simplex virus. J Virol 2001;75:7050–7108. [PubMed: 11435585]
24. Aghi M, Rabkin S, Martuza RL. Effect of chemotherapy-induced DNA repair on oncolytic herpes simplex viral replication. J Natl Cancer Inst 2006;98:38–50. [PubMed: 16391370]

25. Eisenberg DP, Adusumilli PS, Hendershott KJ, Yu Z, Mullerad M, Chan MK, et al. 5-fluorouracil and gemcitabine potentiate the efficacy of oncolytic herpes viral gene therapy in the treatment of pancreatic cancer. J Gastrointest Surg 2005;9:1068–1077. [PubMed: 16269377]

26. Liu TC, Wakimoto H, Martuza RL, Rabkin SD. Herpes simplex virus Us3(−) mutant as oncolytic strategy and synergizes with phosphatidylinositol 3-kinase-Akt targeting molecular therapeutics. Clin Cancer Res 2007;13:5897–5902. [PubMed: 17908985]

27. Maiato H, Rieder CL. Stuck in division or passing through: What happens when cells cannot satisfy the spindle assembly checkpoint. Dev Cell 2004;7:637–651. [PubMed: 15525526]

28. Motwani M, Delohery TM, Schwartz GK. Sequential dependent enhancement of caspase activation and apoptosis by flavopiridol on paclitaxel-treated human gastric and breast cancer cells. Clin Cancer Res 1999;5:1876–1883. [PubMed: 10430095]

29. Wittman S, Bali P, Donapaty S, Nimmanapalli R, Guo F, Yamaguchi H, et al. Favopiridol down-regulates antiapoptotic proteins and sensitizes human breast cancer cells to epothilone B-induced apoptosis. Cancer Res 2003;63:93–99. [PubMed: 12517783]

30. Tao W, South VJ, Zhang Y, Davide JP, Farrell L, Kohl NE, et al. Induction of apoptosis by an inhibitor of the mitotic kinesin KSP requires both activation of the spindle assembly checkpoint and mitotic slippage. Cancer Cell 2005;8:49–59. [PubMed: 16023598]

31. Lin S-F, Gao SP, Price DL, Li S, Chou TC, Singh P, et al. Synergy of a herpes oncolytic virus and paclitaxel for anaplastic thyroid cancer. Clin Cancer Res 2008;14:1519–1528. [PubMed: 18316577]

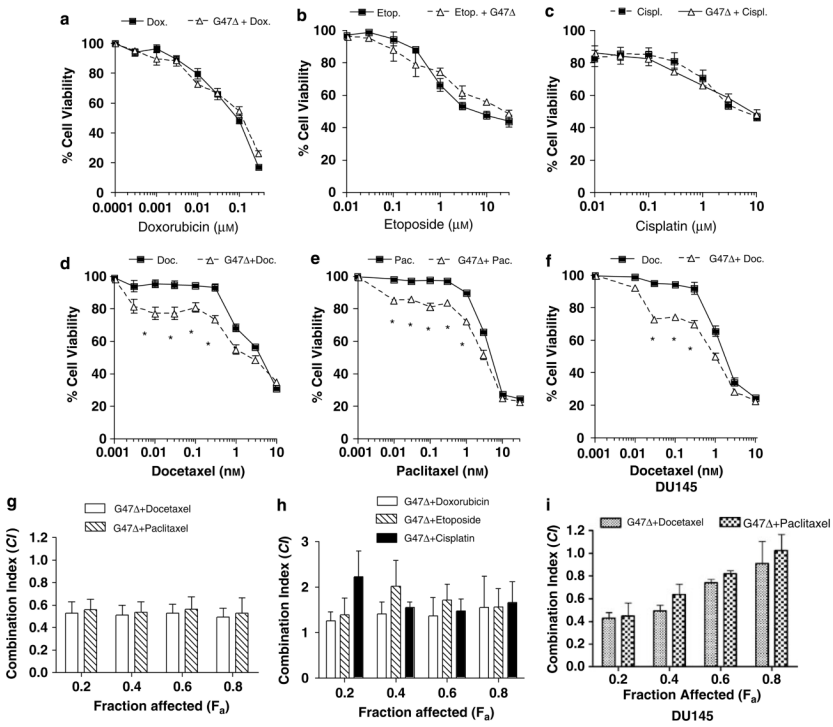

Figure 1.

G47Δ and taxanes synergize to promote augmented LNCaP and DU145 cell killing. (**a**–**f**) LNCaP and DU145 cells were treated with increasing concentrations of doxorubicin (**a**), etoposide (**b**), cisplatin (**c**), docetaxel (**d** and **f**) or paclitaxel (**e**) alone (solid line/black square) or in combination with G47Δ (dotted line/black triangle) at a multiplicity of infection (MOI) of 0.01 (or 0.05 for DU145) for 72 h. MTS assays were performed to determine the extent of cell killing. G47Δ alone resulted in ~10–15% cell death over this same time period and was accounted for to normalize percent cell killing of G47Δ and docetaxel together. Asterisks indicate $P<0.01$, Student's *t*-test. (**g**–**i**) Fraction affected versus combination index (f_a–CI) plots were generated using the method of Chou and Talalay to determine the extent of synergy for either docetaxel or paclitaxel in combination with G47Δ (**g**), or G47Δ in combination with either doxorubicin, etoposide or cisplatin (**h**) in LNCaP cells. Synergy was also assessed in DU145 cells for the combination of G47Δ and either taxane (**i**). Synergistic effects are defined as combination index (CI) values below 0.9. Additive effects are CI=0.9–1.1. Antagonistic effects are CI>1.1. These data represent the average±s.e.m from three independent experiments.

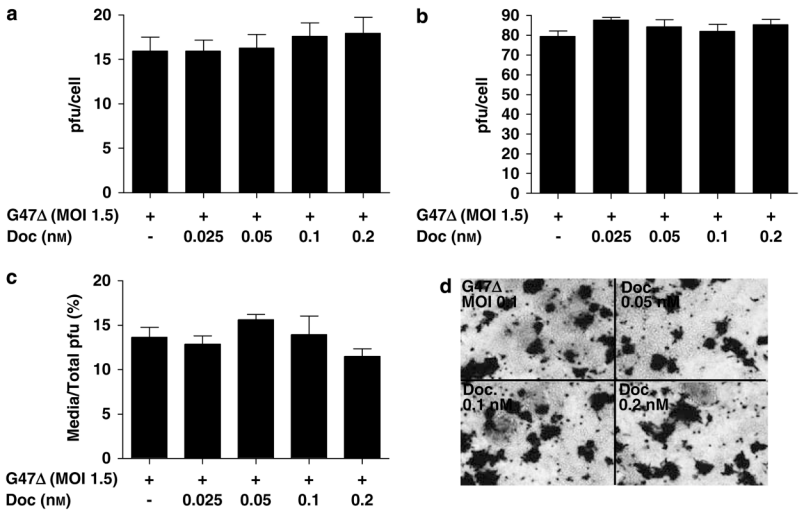

Figure 2.

Docetaxel does not promote G47Δ replication or enhanced cell-free virus in LNCaP cells. (**a** and **b**) Single-step growth curve assays demonstrate that pretreatment with a nontoxic range of docetaxel (0.025–0.2 nM) had minimal influence on G47Δ activity either at 24 (left panel) or at 48 h (right panel) after infection. (**c**) Cell-free virus assays reveal minimal influence of docetaxel pretreatment on G47Δ titers. LNCaP cells were pretreated with the indicated concentrations of docetaxel and 48 h after infection, supernatants and cells were collected separately, titered on Vero cells and the percentage of pfus in the supernatant was determined based on their combined pfus. (**d**) Micrographs of LNCaP cells pretreated with the indicated doses of docetaxel revealed negligible differences in X-gal staining 48 h after infection with G47Δ (multiplicity of infection; MOI 0.1).

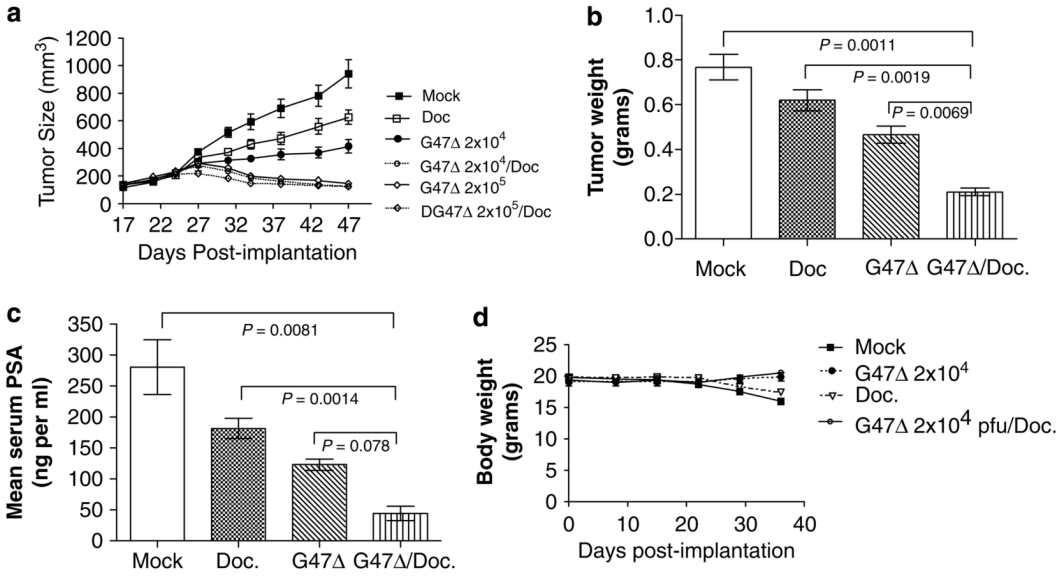

Figure 3.

G47Δ and docetaxel dual-therapy promotes tumor regression in nude mice. (**a**) Subcutaneous LNCaP-derived prostate tumors were established in nude mice and therapy commenced when LNCaP tumors ranged in size from 75–150mm^3. Two intratumoral injections of G47Δ at 2×104 or 2×105 pfu per injection were administered on days 0 and 3 either alone or in combination with three intraperitoneal injections of docetaxel (3mg kg^{-1}) every third day starting on day 4. At day 47, mock versus G47Δ (2×10^4), *P*=0.026; mock versus docetaxel, *P*=0.0422; G47Δ (2×10^4) versus docetaxel, *P*=0.0443; G47Δ (2×10^4) versus G47Δ (2×10^4)/docetaxel, *P*=0.0108; docetaxel versus G47Δ (2×10^4)/docetaxel, *P*=0.001; two-tailed Student's *t*-test. (**b**) Tumor weight and (**c**) prostate-specific antigen (PSA) levels were assessed for either G47Δ (2×10^4), docetaxel or combination treatment groups 47 days after implantation. (**d**) Body weight was also evaluated for all the treatment groups to determine the extent of toxicity of the combination therapy regime. For purposes of clarity, the treatment groups G47Δ (2×10^5) and G47Δ (2×10^5)/docetaxel were omitted from the graph, which were similar in body weight to G47Δ (2×10^4) and G47Δ (2×10^4)/docetaxel.

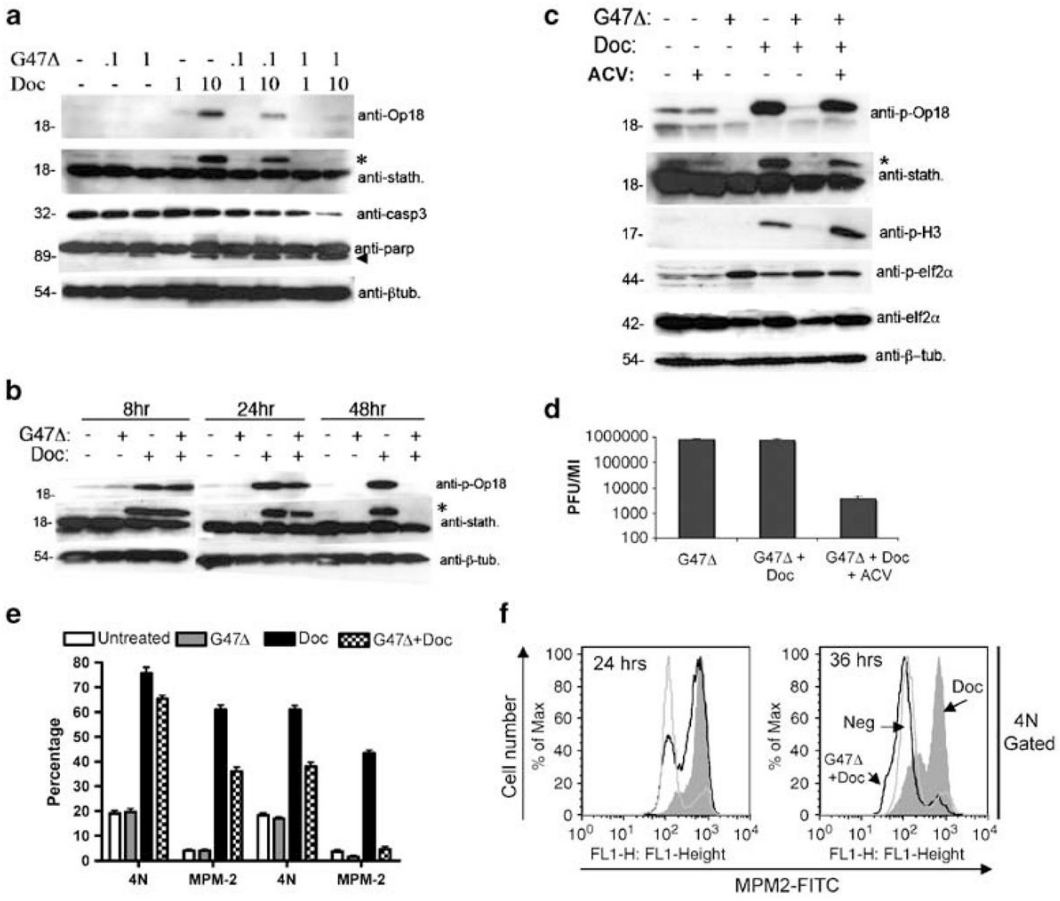

Figure 4.

Effects of G47Δ on Docetaxel-induced mitotically arrested cells. (**a**) Dose-dependent effects of G47Δ on docetaxel-induced op18/stathmin phosphorylation. LNCaP cells either remained untreated (−) or were inoculated with G47Δ (multiplicity of infection; MOI 0.1 or 1) in the presence or absence of docetaxel (1 or 10 nM) for 48 h. Cell lysates were immunoblotted with either anti-op18, which specifically detects op18 phosphorylated on serine-16 (23 kDa) or anti-stathmin, which recognizes both the unphosphorylated (18 kDa) and phosphorylated forms of op18. Asterisk (*) denotes the detection of the phosphorylated form of op18/stathmin using the anti-stathmin antibody. Combination of G47Δ and docetaxel also promotes enhanced cell death as detected by increased caspase-3 (casp3) and PARP cleavage. Arrowhead indicates the 89 kDa fragment of cleaved PARP. An anti-β-tubulin (β-tub.) was included as a loading control. Note that the decreased levels of full-length caspase-3 (32 kDa) reflects its activation. (**b**) Temporal-dependent effects of G47Δ (MOI 1) on docetaxel-induced op18/stathmin phosphorylation. Lysates were collected at 8, 24 and 48 h and immunoblotted with either anti-op18 anti-stathmin or anti-β-tubulin. (**c**) Acyclovir (ACV) attenuates the effects of G47Δ (MOI 1) on docetaxel-induced op18/stathmin phosphorylation. Similar results were obtained when lysates were probed with the mitotic-specific marker anti-phospho-histone-H3 (p-H3). Lysates were also probed with either anti-phospho-eIF2α or anti-eIF2α to show that the effects of G47Δ on docetaxel-induced mitotic block do not influence the phosphorylation status of eIF2α. (**d**) Single burst assays were performed in parallel to demonstrate the effectiveness of acyclovir on G47Δ replication 48 h after infection. (**e**) Cell-cycle analysis on the effects of G47Δ on mitotically arrested cells. LNCaP cells were treated with either G47Δ (MOI 1), docetaxel (10 nM) or their combination and at either 24 or 36 h, the percentages of 4N and

MPM-2-containing populations were determined by two-color PI and anti-MPM-2 antibody staining. Experiments represent the average±s.e.m. of three independent experiments (**f**). The 4N-gated populations were analyzed for MPM-2 staining at 24 and 36 h as a function of treatment groups. Note, by 36 h the majority of the 4N cells lack MPM-2 labeling due to G47Δ infection.

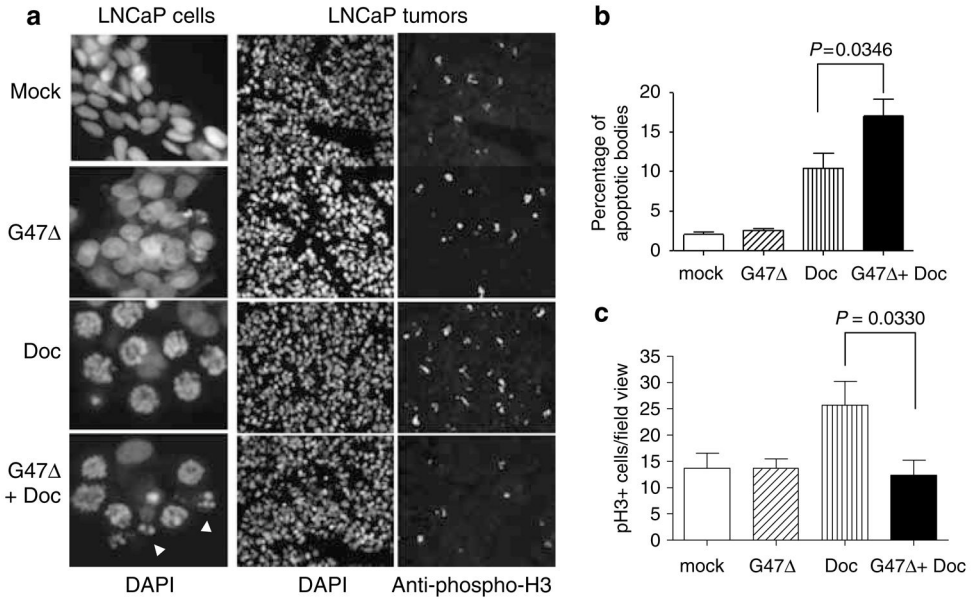

Figure 5.

In vitro and *in vivo* functional analyses of the effects of G47Δ on docetaxel-induced mitotic arrest. (**a**, left panel) G47Δ enhances the formation of fragmented DNA in docetaxel-treated LNCaP cells. Cells were plated in eight-well chamber slides, treated as indicated for ~36 h, fixed and stained with 4′,6-diamidino-2-phenylindole dihydrochloride (DAPI). Nuclear staining was analyzed by fluorescence microscopy and scored for the appearance of apoptotic bodies for each of the treatment groups. The photograph represents one of three independent experiments that gave similar results. White arrowheads indicate fragmented DNA-containing cells. (Middle and right panels) Docetaxel-induced p-H3-expressing cells are diminished by G47Δ treatment in LNCaP-derived tumors. Nude mice harboring LNCaP-derived tumors (n=3) were treated with phosphate-buffered saline (PBS; mock), G47Δ (2×104 pfu), docetaxel (3mgkg^{-1}) or in combination and one day following the last docetaxel injection, tumors were removed, sectioned (5 μM) and immunostained with anti-pH3 antibody followed by a fluorescein isothyocyanate (FITC)-labeled secondary antibody (right panel) and nuclei counterstained with DAPI (middle panel). (**b**) Quantification of LNCaP-containing fragmented DNA. More than 40 fields per slide were scored to obtain the mean±s.e.m. and are representative of three independent experiments. Note that these data are likely to represent an underestimation of the percentage of cells containing fragmented DNA, because LNCaP cells easily detach from the plastic chamber after viral infection and thus are lost from the analysis. (**c**) Quantification of pH3^{+} cells in LNCaP tumors. Data represent the average±s.e.m. of the indicated treatment groups (n=3 per group). At least 10 fields/slide were scored to determine the percentage of pH3+ cells/field view. Two-tailed (paired) Student's t-test was performed to determine P values. White arrowheads indicated cells containing fragmented DNA.